Chapter-4

(Role of particle size and amount of antioxidants on the durability of Al_2O_3-ZrO_2-C)

Chapter 4

Role of particle size and amount of antioxidants on the durability of Al_2O_3-ZrO_2-C

4.1 Motivation

High-duty Alumina-Zirconia-Carbon refractories are most widely used to control the flowing molten steel in the form of slide gate and other functional parts. The oxidation of carbon, however, is always the main drawback of these refractories, which results in an increased porosity and decrease of strength.

One way to reduce this oxidation is by adding non-oxides such as metal, alloy, and carbide, which react with the air and expand, sealing pores.

Initially, non-oxides were added to prevent the oxidation of carbon. It was learned, however, that these non-oxides not only acted as antioxidants, but they also had other effects on the refractory including:

(1) The decrease of carbon loss by the reduction of CO(g) to C(s).

(2) The decline of porosity.

(3) The increase in the modulus of rupture (MOR).

(4) Crystallization of amorphous carbon precipitated from the binder.

(5) Improvement of the oxidation resistance and corrosion resistance by forming a surface protective layer.

Despite being so advantageous, the increase in adding an amount of metal powder also creates the risk of hydration owing to carbides and nitride phases formed in firing process, which leads to the deterioration of the properties. When the added non-oxide changes to an oxide, a volume expansion is generated. To tackle this problem, the present work attempts to study the effect of small quantity of mechanically activated oxidation inhibitors in place of their large amount counterparts.

4.2 Formulation

RAW MATERIALS	**A (1-3)**	**B (1-3)**	**C (1-3)**	**D (1-3)**
Tabular Alumina (0-3 mm)	82, 84	82, 84	82, 84	82, 84
Zirconia	10	10	10	10
Flake graphite (<250 µm)	4	4	4	4
Nano Carbon Black (20 nm)	1	1	1	1
Aluminum metal powder (Al)	1, 3	0	0	0
Boron Carbide (B_4C)	0	1, 3	0	0
Silicon metal powder (Si)	0	0	1, 3	0
Silicon carbide (SiC)	0	0	0	1, 3
Liquid resin (Resol)	+3.50	+3.50	+3.50	+3.50
Powder resin	+0.50	+0.50	+0.50	+0.50

Table 4.1 Formulation Al_2O_3-ZrO_2-C with different antioxidants

A total number of twelve different formulations were introduced to verify whether a decrement in particle size and the mechanical activation of four different antioxidants could prove to helpful in reducing their amount in the alumina-carbon bricks. To do this samples containing 1wt% as received, 1wt% mechanically activated and a tradition 3wt. wt. The aluminum metal powder as oxidation inhibitors was formed; these were termed as A1, A2 and A3 respectively. Similarly, B, C, and D series samples were designed which were comprised of boron carbide, silicon metal powder, and silicon carbide respectively. The A1, B1, C1, D1 and A2, B2, C2, D2 formulations had an 84 wt% tabular alumina; whereas, A3, B3, C3 and D3 samples had an 82 wt% tabular alumina.

4.3 Results and Discussion

In zirconia ceramics, the stress-induced phase transformation from the tetragonal to the monoclinic phase is considered to be the main toughening mechanism. To obtain high values for bending strength and fracture toughness in these materials, the contribution of transformation toughening should be maximized. Ceria stabilized zirconia (CeSZ) ceramics possess distinct advantages over other conventional structural ceramic materials because of their better thermal stability in moist environments, a wider range of solid solubility in the tetragonal region.

Consequently, ceria stabilized zirconia ceramics have been investigated extensively for structural applications. The grain size and microstructure of these materials are difficult to control in the conventional technique. Gelation and co-precipitation process is a promising candidate for the production of CeSZ particles giving better control over size and shape of the synthesized nanopowders.

To prepare this, AR grade $ZrOCl_2.8H_2O$ and $Ce(SO_4)_{2.}4H_2O$ were dissolved in deionized water with vigorous stirring and mild heating to give 8 mole % ceria stabilized zirconia [$(Zr)_{0.92}(Ce)_{0.08}O_2$]. For the preparation of gel, ammonia solution was added dropwise, and pH of the solution was maintained over 9. A point was reached when the gel became fully viscous, and the process of stirring was stopped due to the viscous nature of the gel. This gel was oven dried at 80 °C and finally calcined at 750 °C for 5 h to give super fine ceria stabilized zirconia. Applying the Scherrer's formula, crystallite size from the {111} diffraction plane is evaluated to be 18 nm. A 72% tetragonal phase was retained in calcined powders as calculated by Garvie-Nicholsan equation:

$$f_m = \frac{C[I_m(111)+I_m(-111)]}{I_t(111)+C[I_m(111)+I_m(-111)]} \qquad (4.1)$$

Where C is a constant = 1.381, when Cu Kα radiation was used.

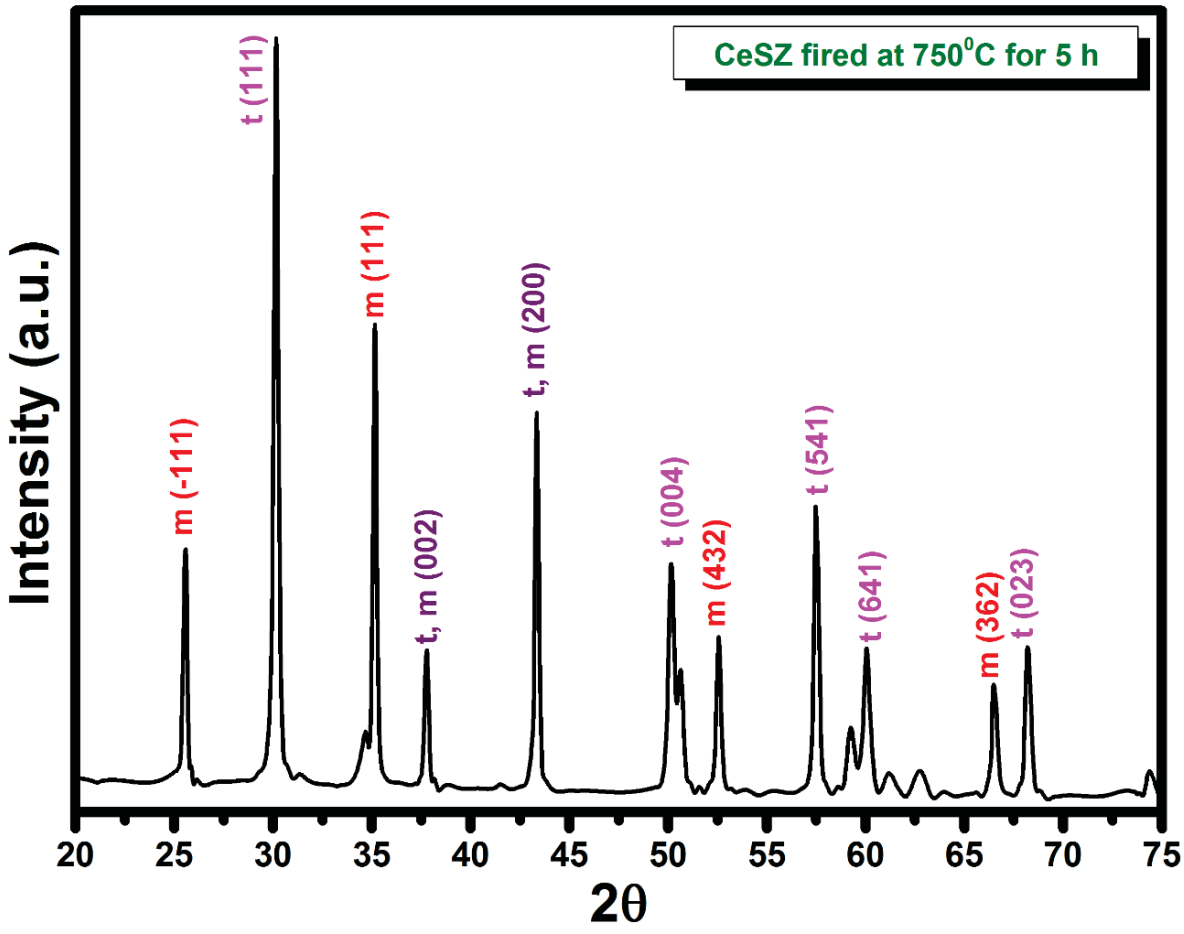

Fig 4.1 XRD plot of gelation and co-precipitation processed 8 mol% ceria stabilized zirconia calcined at 750 °C for 5 h.

This amount of tetragonal zirconia helps to accommodate more stress due to its martensitic transformation mechanism. During the application when a stress is applied on this zirconia containing refractory, it transforms into monoclinic and stress gets distributed to a larger surface area. The formation of micro-cracks also helps deflect the further crack propagation.

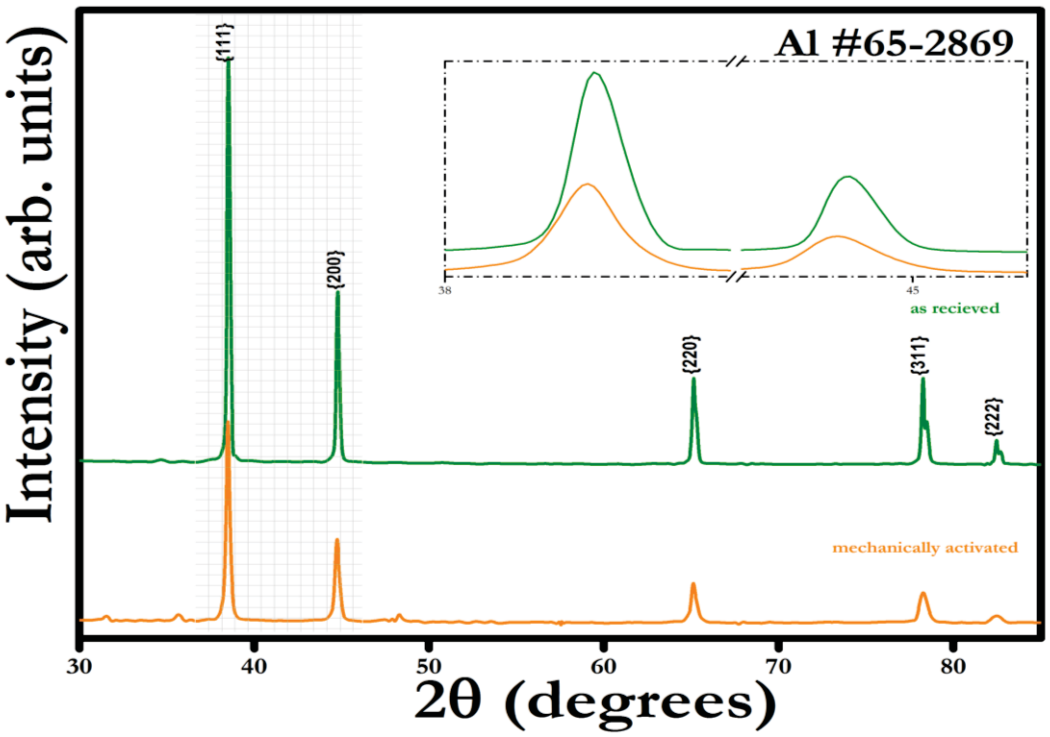
Al #65-2869
Intensity (arb. units)
{111}
{200}
{220}
{311}
{222}
as recieved
mechanically activated
30
40
50
60
70
80
2θ (degrees)

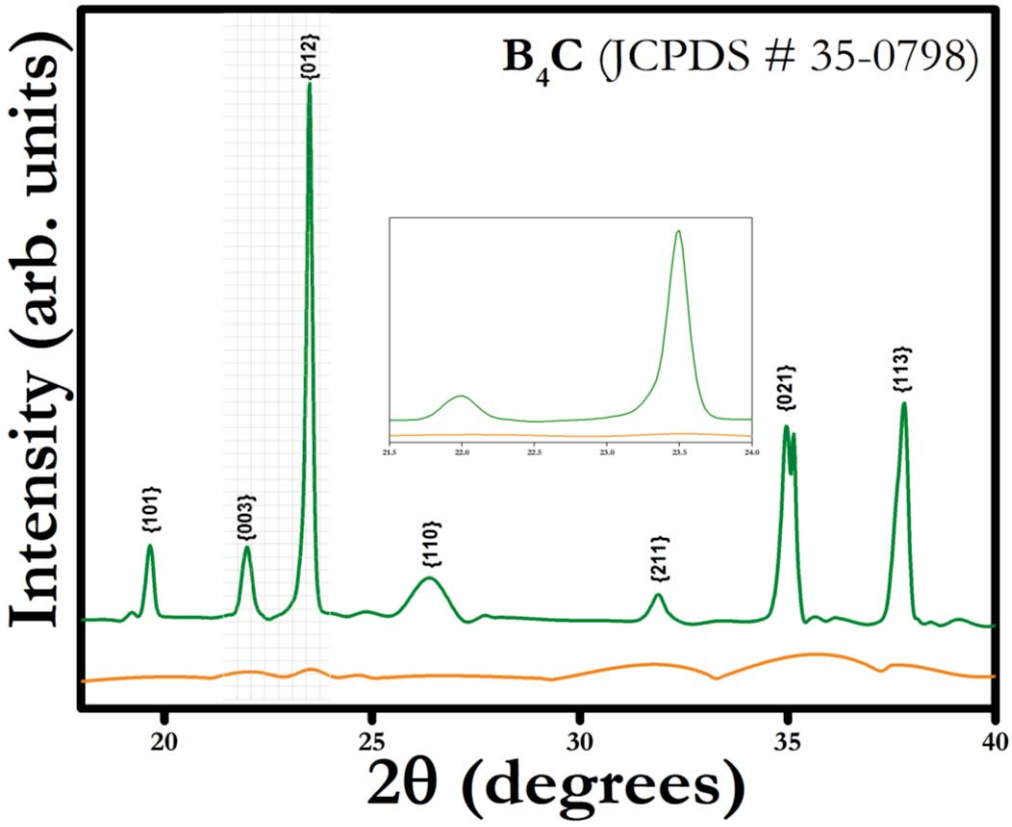
B4C (JCPDS # 35-0798)
Intensity (arb. units)
{012}
{101}
{003}
{110}
{211}
{021}
{113}
20
25
30
35
40
2θ (degrees)

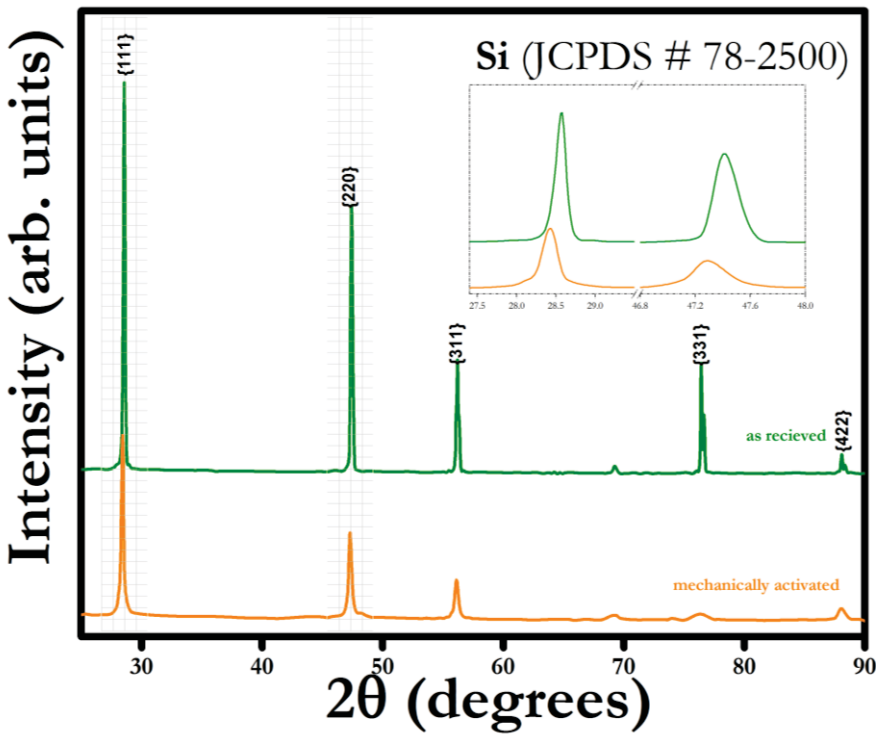

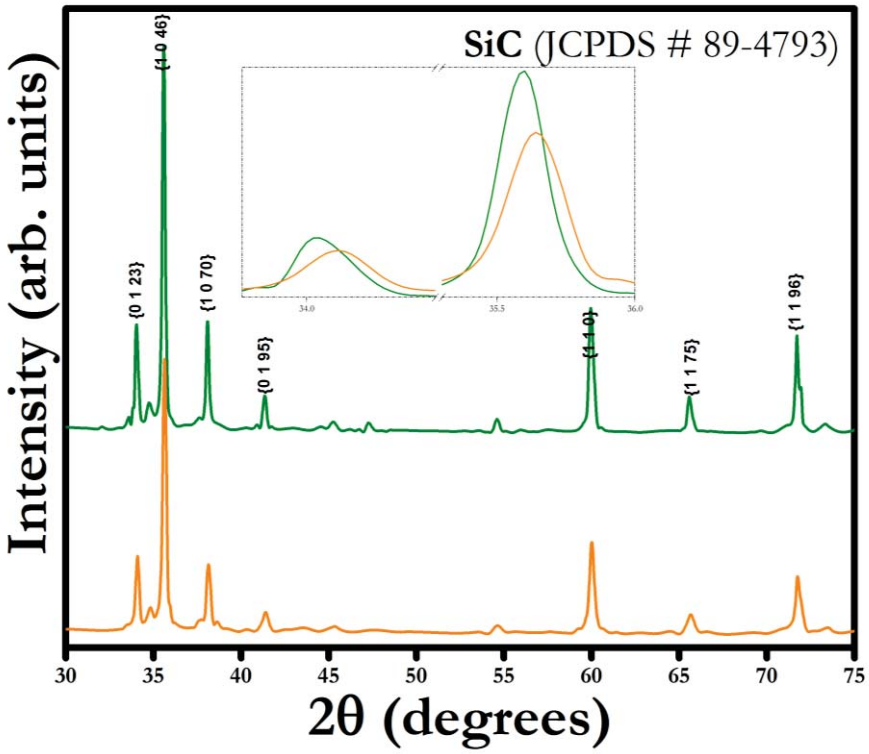

Fig 4.2 XRD plots 3h, 600 rpm milled (a) Al, (b) B_4C, (c) Si and (d) SiC

The XRD peak broadening is in direct relation with the structural anisotropy. The XRD method is a local, quantitative and selective technique, which made particularly possible to evaluate intensity and distribution of microscopic internal stresses in deformed microstructures. Here, the particle size reduction is accompanied by a general broadening of the peaks (increased FWHM). A significant amount of decrease in crystallite size is observed in B_4C and Al. The inhomogeneous structures give internal stresses at different scales, which strongly influence the superficial mechanical properties. The presence of significant peaks even after intensive milling in SiC and Si indicate their high milling resistance and mechanical strength of their sub-micrometer particles. It may be noted that the peak broadening has a good linear relationship with the yield strength.

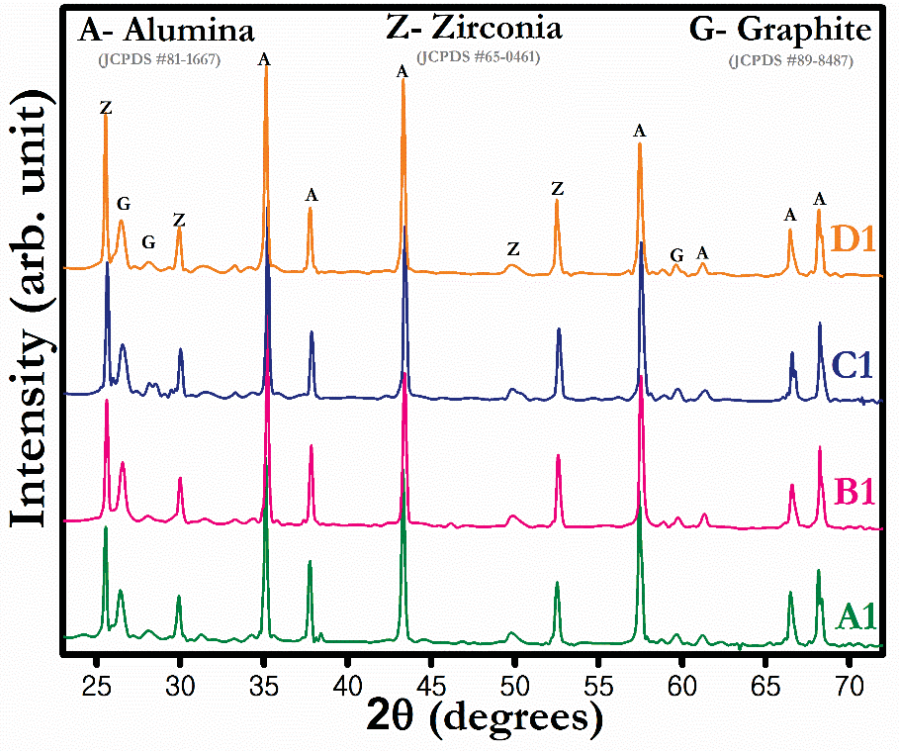

Fig 4.3 XRD pattern of samples coked at 1400°C for 3h

As formulated alumina had the major crystalline peaks, while zirconia and graphite form rest other peaks. The detection limit of XRD is about 5 wt%. Since the oxidation inhibitors were added to a concentration of ≤3 wt%, it was not possible to observe their presence. Hence, none of the peaks corresponding to metal powders or the carbides are evident in the above plot. The secondarily formed carbides are also not detected in the above plot which indicates that even their presence was lower than five weight percent. The peaks of alumina were identified with the JCPDS card number 81-1667. Similarly, peaks of zirconia and graphite matched exactly with the JCPDS card numbers 65-0461 and 89-8487 respectively.

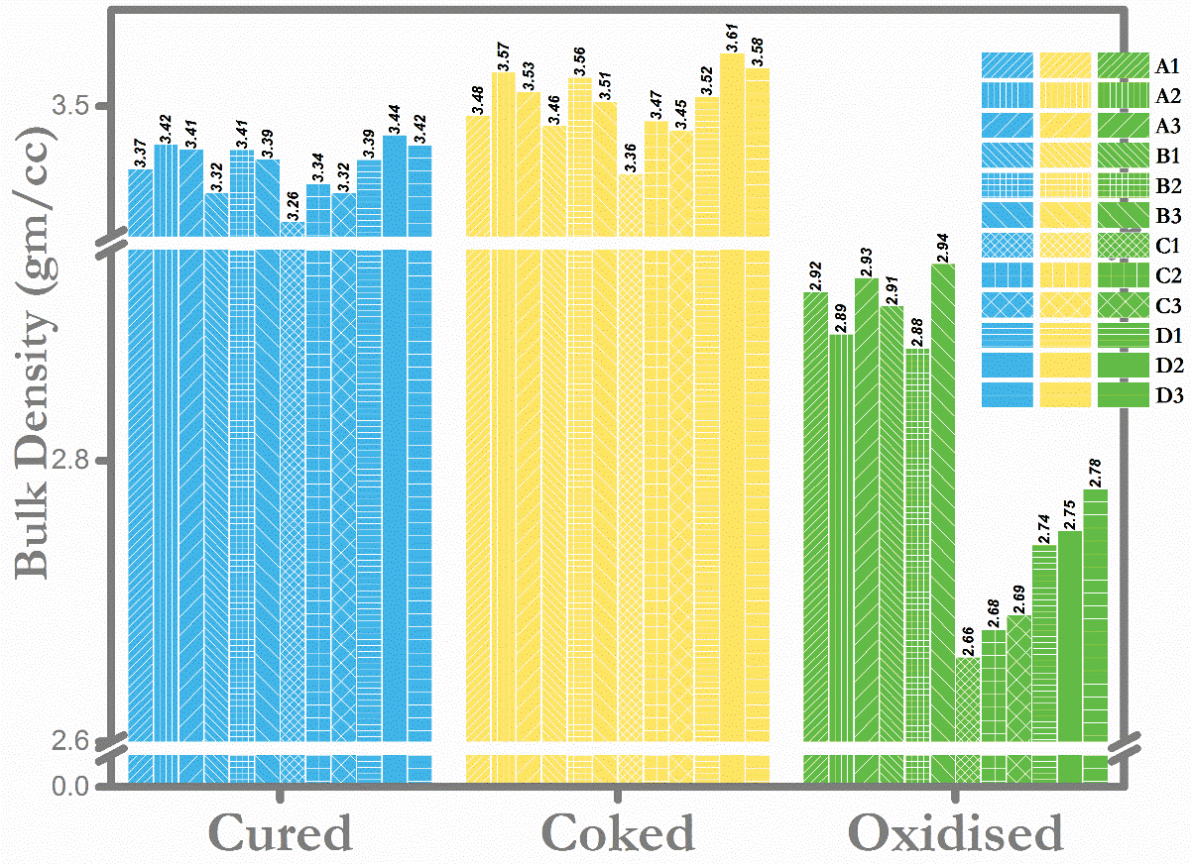

Fig 4.4 Bulk density as a function of heat treatment conditions

The difference in the bulk density of all cured samples is not much significant as the no reaction takes place between the components at this temperature. Their values are high due to the resin forming a complex network structure and filling up the open pores. After the coking, reactions between oxidation inhibitors and gaseous constituent CO triggered the formation of expansive phases (oxides, carbides) which further helped in pore filling and densification; this process was more pronounced in aluminum, boron carbide and silicon carbide containing samples. However, more expansion in C2 series gives a side effect on the bulk density even in the case of remarkable weight gain. The formation of low melting phases like aluminum borate increase the density by a mechanism of liquid phase sintering and filling up the open pores and forming a dense layer on the brick surface. Thus oxidation ingress is restricted as well.

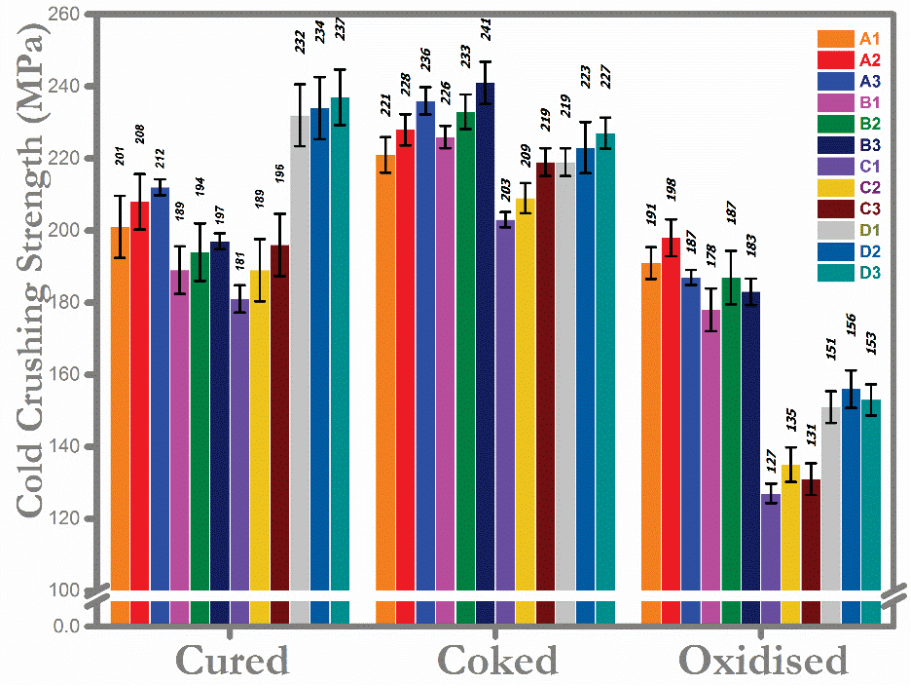

Fig 4.5 Crushing strength as a function of heat treatment conditions

In the cured samples containing silicon carbide, a highest crushing strength is observed. It might be due a better crack deflection than other specimens. This high strength achieved, slightly decreases due to oxidation tendency of these samples and evolution of volatile phenolic residues. The decrement of the amount of carbon and in turn decreased bulk density might also be a major cause behind this phenomenon.

The Al and B_4C containing samples present better residual strength after oxidation. In the samples containing silicon and silicon carbide, there is a rapid reduction of crushing strength after oxidation. It shows their inefficacy to prevent carbon oxidation. However, mechanical activation did help a bit in retaining carbon. This is visible in C2 and D2 series samples which resist higher uniaxial pressing forces, thereby, presenting better-crushing strength values as compared with their C1, C3, and D1, D3 counterparts.

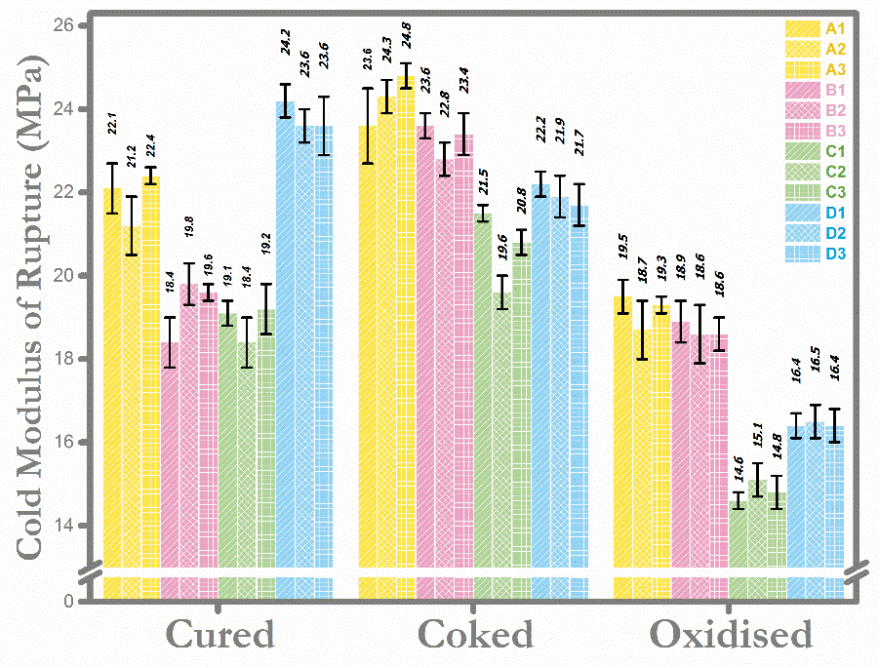

Fig 4.6 Bending strength as a function of heat treatment conditions

Generation of secondary phases in Al and B_4C containing samples led to the formation of stronger bonds and increased samples stiffness. Carbides are excellent additives because they create deposits as a free carbon in a refractory. Potential advantages of whisker forming/containing additives include more efficient crack deflection and superior load-carrying capacity, which is quite evident from the modulus of rupture values.

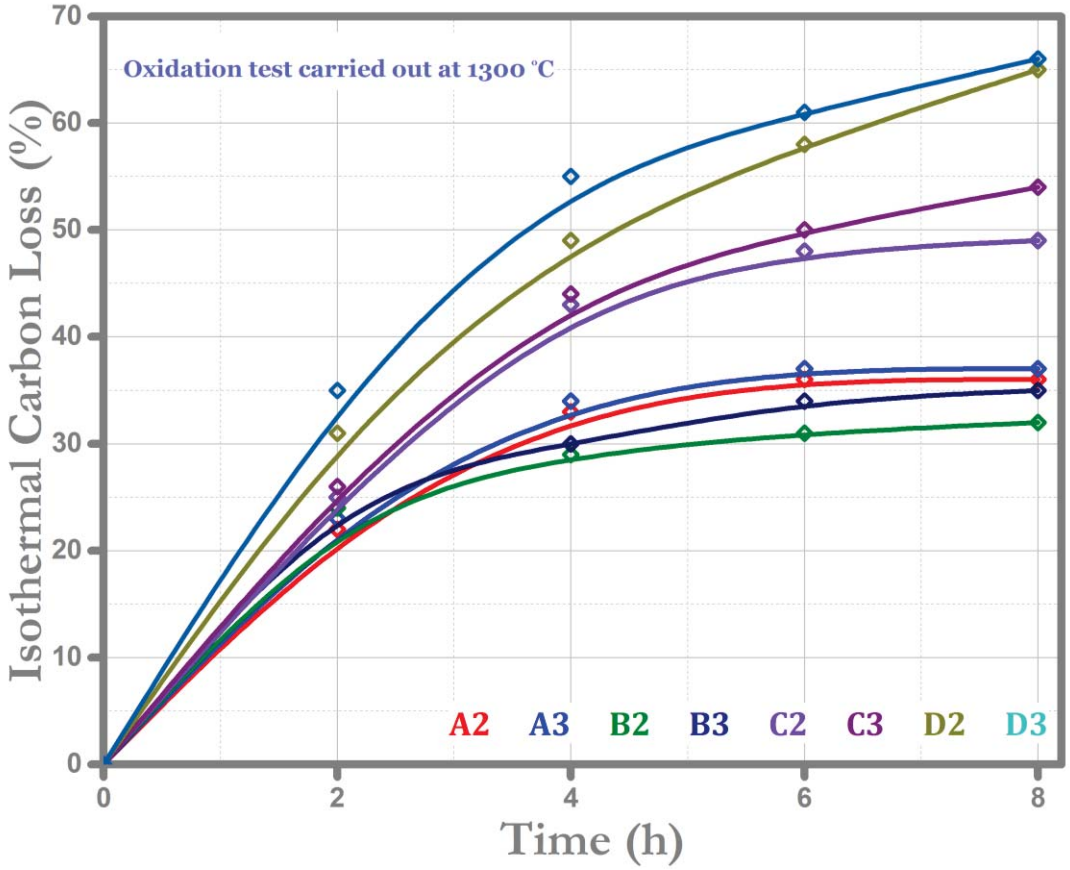

Fig 4.7 (a) Carbon loss as a function of dwell time at 1300°C

Carbon loss curves showed that Al, B4C and somewhat Si antioxidant added specimens had similar results at 1300°C, excluding the specimen with SiC addition.

$$\textbf{\textit{Carbon loss wt\%}} = \frac{\boldsymbol{m1-m2}}{\boldsymbol{m3}\times(\%\boldsymbol{G})} \times \mathbf{100} \qquad (4.2)$$

Where m1 is wt of coked sample, m2 of oxidized and m3 of cured.

The B_4C was the most efficient antioxidant at this temperature and SiC was the least efficient. The only grace was the possible formation of oxygen-derived silica melt which might have acted as a coating agent and prevented complete oxidation. There is also a limiting value of the isothermal carbon loss % after four hours of continuous oxidation. This value is much less in the boron carbide containing samples (~32 wt%) followed by aluminum containing samples (~35 wt%).

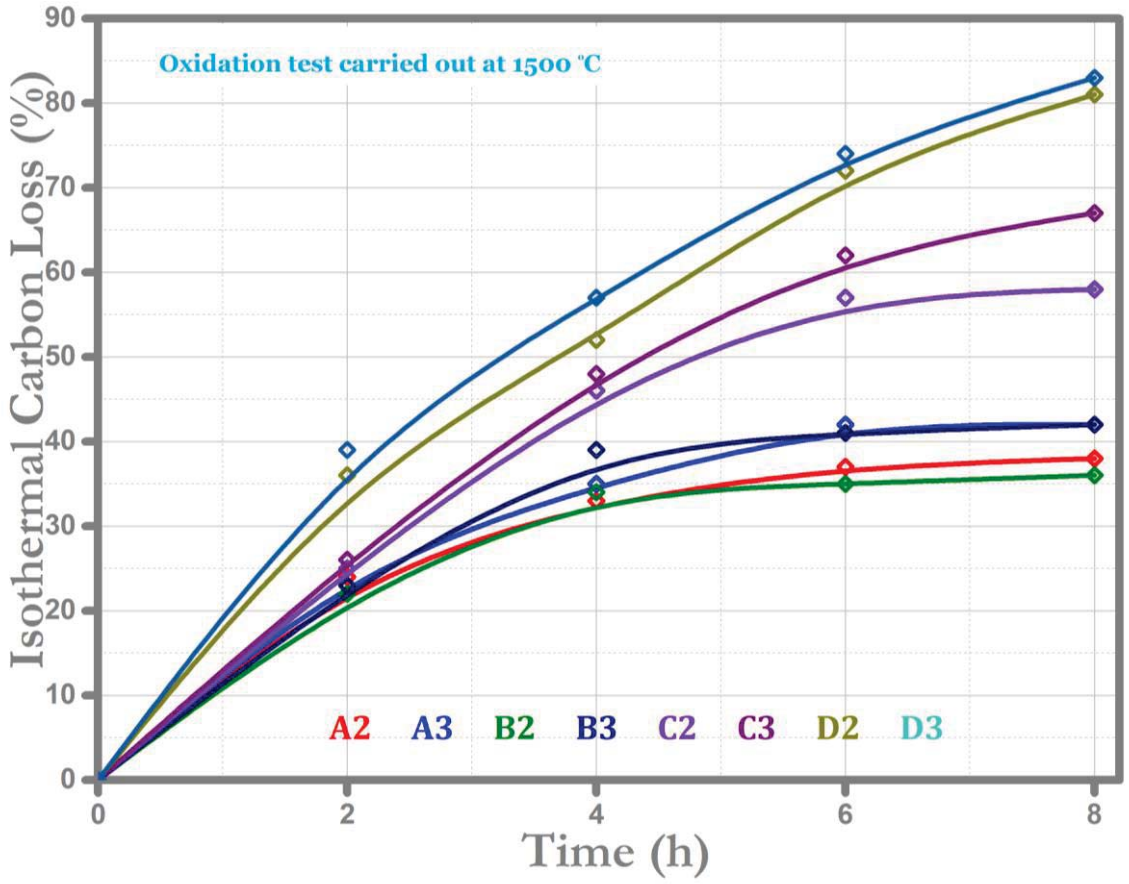

Fig 4.7 (b) Carbon loss as a function of dwell time at 1500°C

Changes in the carbon loss of refractories at 1500°C display that the activated B4C addition had an excellent effect on the oxidation resistance even at this temperature, followed by Al. The degree of oxidation of activated Si-containing sample was different at this temperature as the formation of secondary phases helped it to retain some carbon more than unmilled Si-containing samples. The SiC added samples oxidized and were the worst as an antioxidant. Here again a tendency of slow and limited oxidation after four hours can be envisaged; this effect is more prominent in the A2 and B2 samples. A slow but steeper isothermal carbon loss is visible in the silicon and silicon carbide containing samples.

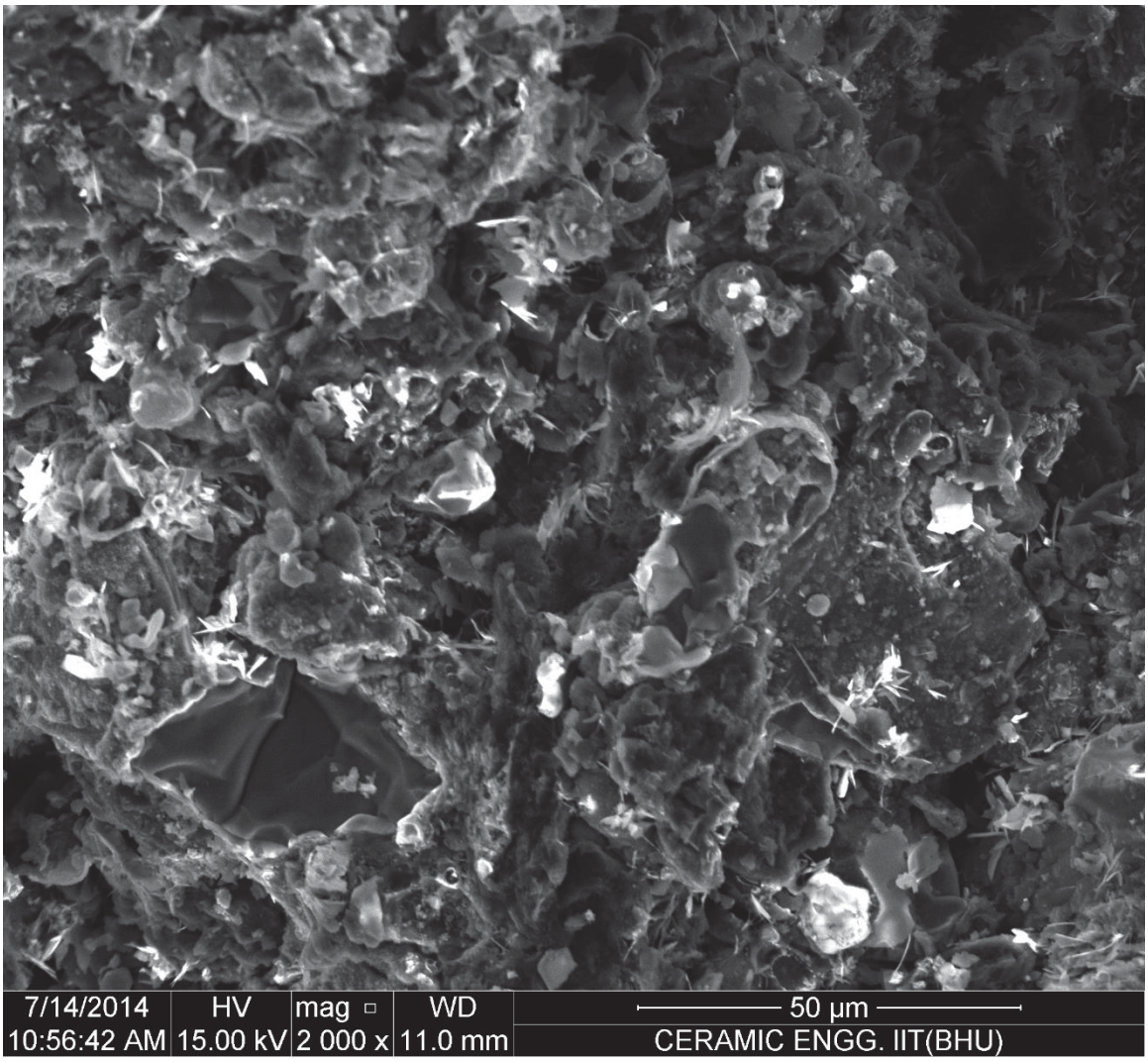

Fig 4.8 (a) SEM of A2 coked at 1400°C

The Al oxidizes rapidly after fabrication and forms a thin Al_2O_3 layer. This thin layer can contain the liquid aluminum for a while until it breaks and releases the molten aluminum. The Al melts at around 660°C; this liquid phase suppresses the diffusion of the oxygen to the refractory at the exact time when carbon oxidation starts. This molten metal further forms Al_4C_3 whiskers which further strengthens the structure.

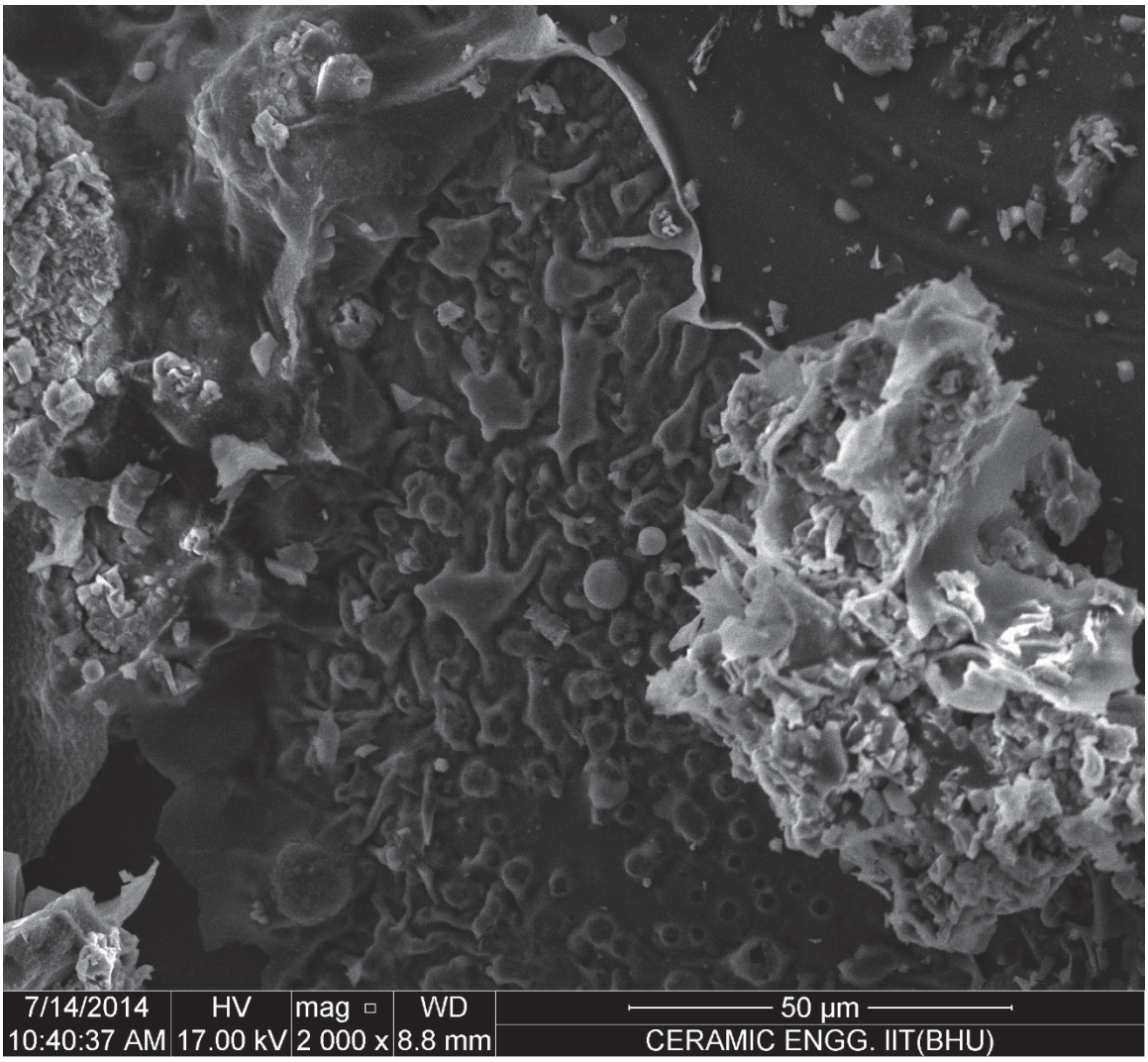

Fig 4.8 (b) SEM of B2 coked at 1400°C

It was observed that the B4C was a much more efficient antioxidant because the $2Al_2O_3 \cdot B_2O_3$ is an excellent oxygen barrier above its melting temperature. It is assumed that the liquid aluminum-borate fills up the open pores and forms a thin film layer on the brick surface so that oxygen cannot diffuse into the refractory matrix. It favors sintering of the structure and leads to improvement of material stiffness and mechanical strength.

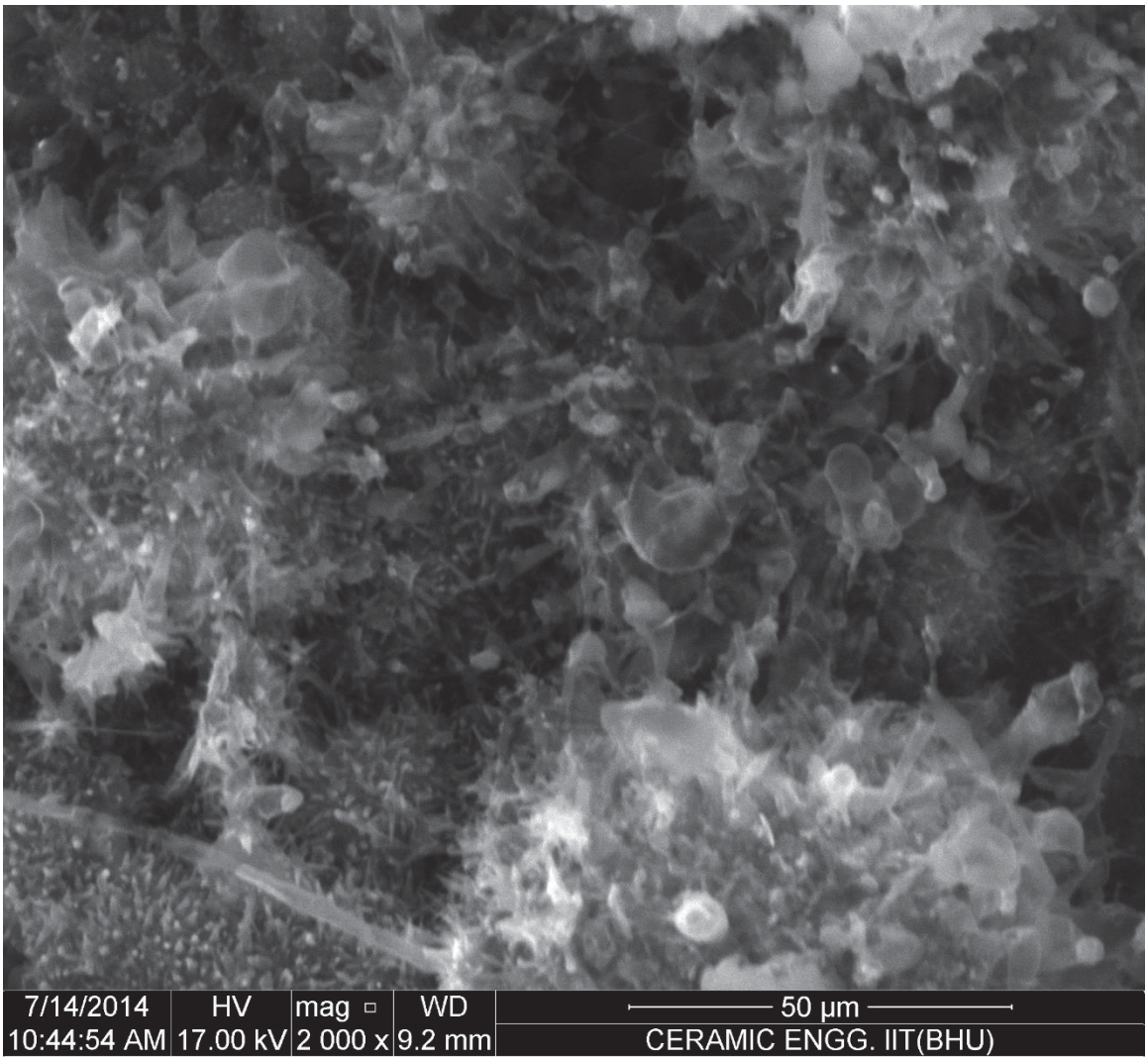

Fig 4.8 (c) SEM of C2 coked at 1400°C

Formation of carbide phases (as observed in microstructure) presents the constant weight gain tendency even though carbonization of the binders causes weight loss of all samples. Si first reacts with C to form SiC whiskers which then reacts with CO to form SiO_2(s). This SiO_2 then reacts with Al_2O_3 to form mullite. Strengthening occurs when the load gets transferred to the whisker. The stress distribution in a test bar subjected to a bending moment is such that a whisker is lying at right angles to the crack plane at the point of

fracture, the maximum bending stress in the whisker will occur in the crack plane.

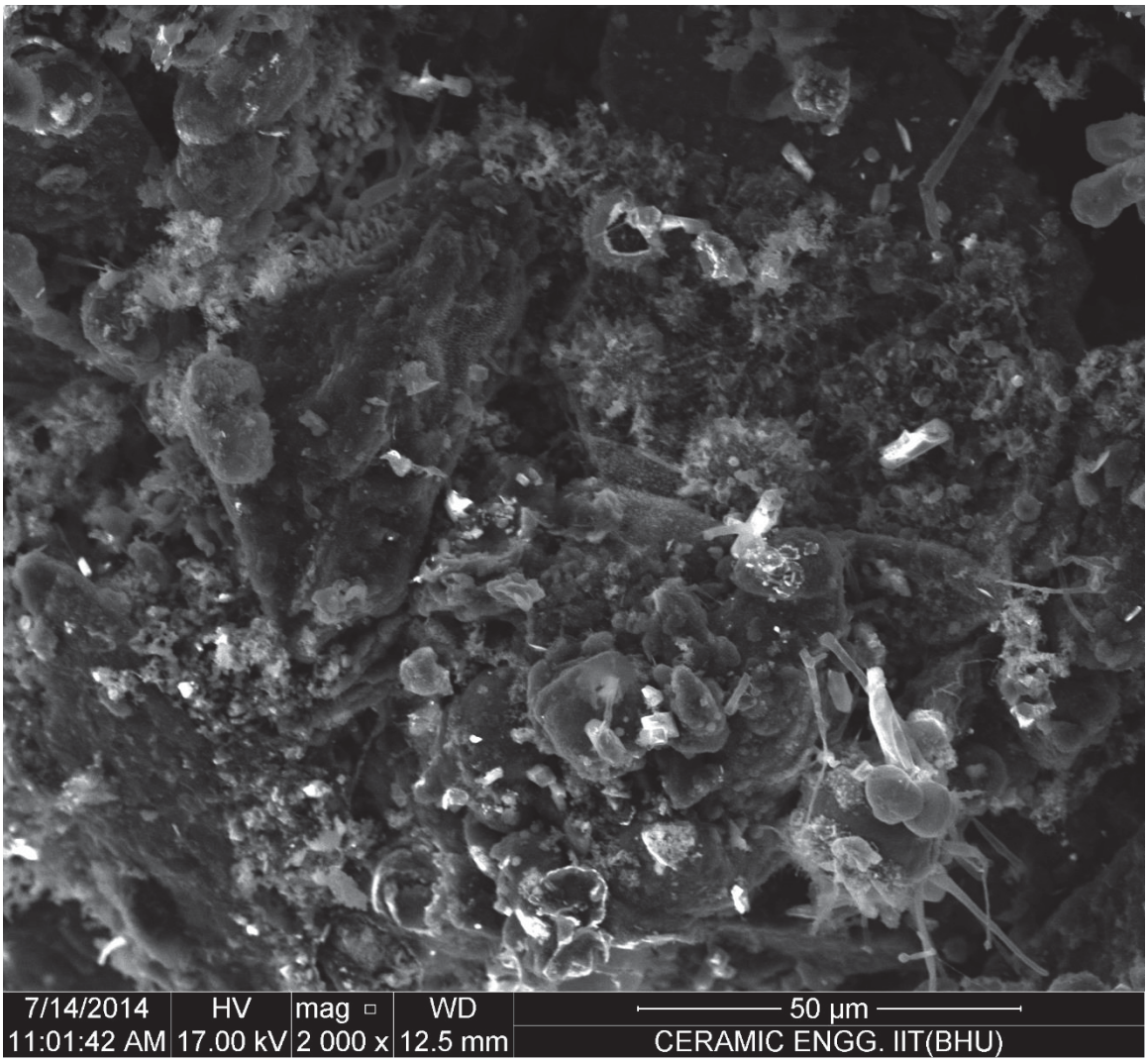

Fig 4.8 (d) SEM of D2 coked at 1400°C

The α-silicon carbide itself is very resistant to oxidation till 1400°C, and it seldom gets oxidized before. β-SiC, on the other hand, is slight inferior carbide and its oxidation starts at a much lower temperature. The antioxidant added was of α grade; hence, it could not prevent much oxidation although it acted as an excellent reinforcement by crack bridging and pullout mechanism.

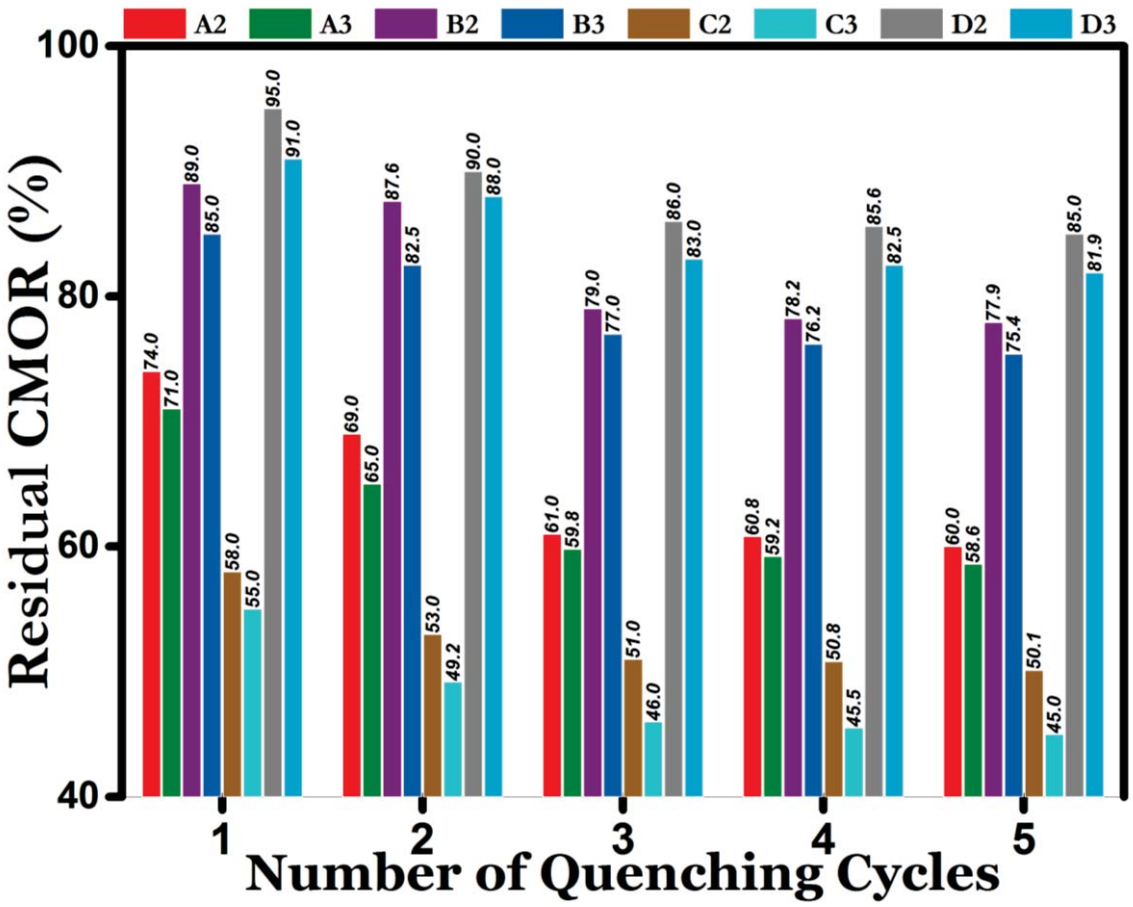

Fig 4.9 TSR as %CMOR retention

After each cyclic thermal shock, a little decrement in residual CMOR value was observed for each sample. Samples containing B_4C and SiC subsequently retained a constant strength even after five such consecutive cycles. Thermal shock damage is more evident in Si and Al containing samples. This may be correlated to the mean free path, which was greater in carbide containing samples than that of carbide forming products because of the smaller dimensions of the later phase.

4.4 Summary of Results

B_4C was the most effective antioxidant in both series samples by forming a protective glassy layer over the carbon. The oxidation resistance values of Al and B_4C containing bricks were similar at 1%. However, there were considerable differences in the 3% samples. The second most effective antioxidant was the Al. Formation of aluminum carbide in the oxidized areas restricted the further oxygen ingress into the bricks by filling up the open pores and forming a dense zone in the oxidized areas. Volume expansion and cracks were observed in refractories containing 3% Al which may be due to hydration of Al_4C_3. The Si addition was not as effective as B_4C. The SiC was the least effective antioxidant in both series, although it acted as highest strengthening agent as compared to others. It was hence deduced that mechanical activation has an active role in oxidation protection and in decreasing the amount of antioxidants in the case of Al and B_4C addition, but it did not affect much the Si, and SiC added samples.